H. C. Lim et al.

Electrodeposition of Zinc Oxide Nanowires as a Counter Electrode in Electrochromic Devices

Hong Chul Lim,[†,‡,§] Eunji Park,[‡,§] Ik-Soo Shin,[‡,*] and Jong-In Hong[†,*]

[†]*Department of Chemistry, Seoul National University, Seoul 08826, Republic of Korea.*
E-mail: jihong@snu.ac.kr
[‡]*Department of Chemistry, Soongsil University, Seoul 369, Republic of Korea. *E-mail: extant@ssu.ac.kr*
[§]*These authors contributed equally to this work.*

Electrochromic devices (ECDs) based on electrochromism are considered suitable for use in various fields including smart windows, car mirrors, and optical display owing to the low power consumption and high coloration efficiency characteristics.[1,2] Electrochromism is modulation of optical property caused by the redox process of an electrochromic (EC) material, which involves intercalation/deintercalation process of ions in the lattice.[3–5] In electrochemical view point, a fast and reversible redox property of EC material is mostly required to be employed in ECDs.[6,7] However, appropriate choice of a complimentary material which undergoes the opposite electrochemical process to the redox process of the EC material is also one of the importance condition.[8] Therefore, in typical two-electrode-system ECDs, a counter electrode (CE) involving the complementary material should have larger (or at least the same) surface area and faster redox reaction property than those of the working electrode (WE) of the EC material in order not to limit the redox process at the WE. Otherwise, overvoltage is formed during the electrochemical reaction in the ECDs, leading to the degradation of ECDs performance. Relatively large overvoltage that is the net reaction voltage should be applied to operate the device, and it eventually results in degradation of the ECDs performance.[9,10] To overcome this problem, various nanostructured metal oxide, such as titanium oxide (TiO_2),[11] nickel oxide (NiO_2),[12] and tungsten oxide (WO_3)[13] were used as the complementary layer at the EC, and these CE could provide large specific surface area and short charge transport distance for redox process supporting high-performance ECD.[14,15] The metal oxides, however, generally require a high-temperature annealing process for controlling the lattice structure and are expensive material with high production costs.[16–19] Nanostructured zinc oxide (ZnO) is one of the potential materials for complementary layer in the ECDs. It provides a large surface area and high electrical conductivity as well as easy fabrication process. Although nanostructured ZnO nanowires (NWs) has been studied in many fields, including field-effect transistor, dye-sensitized solar cell, and organic photovoltaic as

transparent conductors,[20–22] there have been only a few studies on ECDs.[23,24]
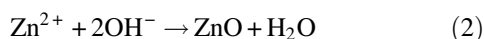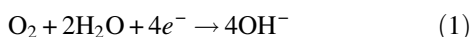
In this study, we report the electrodeposition of ZnO NWs on indiumtin oxide (ITO)/glass substrate and their application as an ion storage CE in ECD. The ECD consists of two ITO electrodes. The WE had the electrodeposited Prussian blue (PB, $KFe^{III}[Fe^{II}(CN)_6]$) thin film as the EC material. The two types of the CE such as a bared ITO electrode and the ITO electrodeposited with ZnO NWs were employed. As a result, the ECD with ZnO NWs thin film at the CE showed drastically improved coloration efficiency and a good cycling life compared to those from the other control.

As the electrochemical operation of the ECD is very similar to those of thin-film batteries, the ion storage capacity of the CE is one of the important requirements.[25,26] The electrodeposition bath consisted of zinc chloride (ZnCl) as a precursor and potassium chloride (KCl), and then ZnO NWs was fabricated on the ITO electrode. The solution in the bath was saturated with oxygen molecules (O_2), and slight O_2 bubbling was maintained throughout the electrodeposition process. We prepared ZnO NWs thin films under various temperature and concentration conditions of the solution of ZnCl and KCl. The concentration of KCl affected the growth of ZnO NWs. As the KCl concentration increased, growth of ZnO NWs slowed, as depicted in Figure S1 (Supporting Information). KCl may interfere with ZnO growth on the surface of ITO owing to the strong adsorption behavior of chloride anions (Cl^-).[27] The growth pattern of ZnO NWs was investigated under various temperature conditions on the deposition solution containing 5 mM $ZnCl_2$ and 0.1 M KCl. Figure S2 shows scanning electron microscopy (SEM) images of the top-view of ZnO NWs array according to the conditions of electrochemical deposition on ITO/glass substrate. The shape and size of the ZnO NW structure were varied depending on the deposition temperature. Thin wave-like ZnO structures were observed at room temperature condition (Figure S2(a)). Interestingly, platelet-like and nanowire structures of ZnO
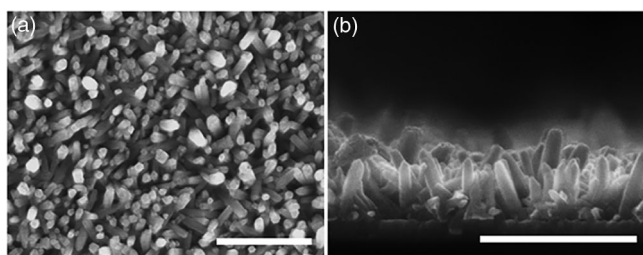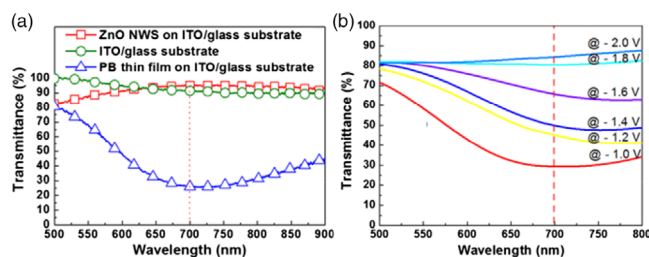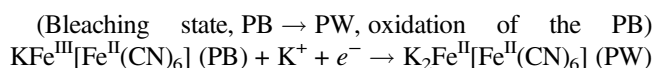
Figure 1. SEM images of the ZnO NWs array electrodeposition grown on the ITO/glass substrate. (a) Top view and (b) cross-sectional view images of ZnO NWs. The condition of electrodeposition is 5 mM $ZnCl_2$ and 0.1 M KCl with O_2 bubbling at 70°C for 1000 s. Scale bar is 1 μm.

Figure 2. (a) Optical transmittance spectra of the samples (line with rectangle symbols: ZnO NWs on ITO/glass substrate, line with circle symbols: ITO/glass substrate, and line with triangle symbols: PB thin film on ITO/glass substrate) and (b) optical transmittance study of the PB thin films at various potential biases from −1.0 to −2.0 V with steps of −0.2 V.
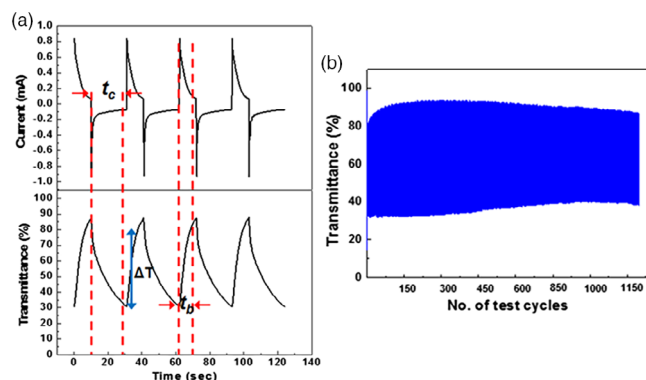
were observed simultaneously at 50°C (Figure S2(c)). It is caused by the competition of ZnO growing in different directions on the ITO substrate. The platelet-like shape is due to the coalescence of neighboring nucleation sites from close-packed grains.[28,29] At 70°C, ZnO NWs grew uniformly, as shown in Figure 1. The ZnO NWs with a height of 400 nm exhibited epitaxial growth of hexagonal the Wurtzite structure.[30] It is because the solubility of O_2 and the nucleation of ZnO are affected by the temperature of the electrodeposition bath.[31,32] The mechanism of the growth of ZnO NWs structures proposed in the previous reports is as follows[24,33]:

$$O_2 + 2H_2O + 4e^- \rightarrow 4OH^- \tag{1}$$

$$Zn^{2+} + 2OH^- \rightarrow ZnO + H_2O \tag{2}$$

As a result, it is believed that the ZnO NWs thin films obtained with conditions of 5.0 mM $ZnCl_2$ and 0.1 M KCl at 70°C could provide a large surface-to-volume ratio for high storage of counter ions in ECDs. The X-ray diffraction patterns of ZnO NWs thin film and bare ITO samples performed to investigate the crystallinity of ZnO NWs (Figure S3). The two peaks related to strong (101) and weak (002) plane peaks from the ZnO NWs thin-film implied that the ZnO NWs grown by electrodeposition process is oriented along 101 direction with crystallinity.[28]

To evaluate the ZnO NWs thin films for the ion storage layer of CE in ECDs, Prussian blue ($KFe^{III}[Fe^{II}(CN)_6]$, PB) as the EC material was prepared by electrodeposition.[34] The color change of the ECDs is caused by the optical modulation of the PB thin film during its redox process. As shown in Figure S4, the morphology and thickness of PB thin film are confirmed by SEM. The color change of PB thin film occurs upon the intercalation/deintercalation of counter ions (potassium cation, K^+) into the lattice channel of the PB structure during the redox reactions.[35] The redox reaction during the EC process is expressed as below:

(Bleaching state, PB → PW, oxidation of the PB) $KFe^{III}[Fe^{II}(CN)_6]$ (PB) $+ K^+ + e^- \rightarrow K_2Fe^{II}[Fe^{II}(CN)_6]$ (PW)

(Coloration state, PW → PB, reduction of the PW) $K_2Fe^{II}[Fe^{II}(CN)_6]$ (PW) $- K^+ - e^- \rightarrow KFe^{III}[Fe^{II}(CN)_6]$ (PB) where, PB and PW mean Prussian blue in the coloration state and Prussian white in the bleaching state, respectively. The electrochemical behavior of the PB thin films was investigated using cyclic voltammetry (CV) experiments. The CV experiments were performed in an aqueous solution containing 0.5 M KCl in a three-electrode electroanalytical cell, consisting of a PB thin film at WE, a Pt foil CE, and a Ag/AgCl reference electrode. The electrochemical reaction of PB thin films showed three redox reactions, as shown in Figure S5. When the PB thin film underwent reduction, the bleaching state from PB to PW was observed around −0.16 V. In addition, when the PW underwent oxidation around +0.4 V, the coloration state of PB observed again. As the PB film could be further oxidized around +1.05 V, the color change from PB to Berlin green (BG) was finally observed. The transmittance change of PB thin films according to various applied voltages was measured at 700 nm. As the transmittance value of as-prepared ZnO NWs thin film is higher than that of bare ITO in that area (Figure 2(a)) so that ZnO NWs provides no interference with the observation of PB color change. Figure 2(b) shows that the transmittance of the PB thin film enhanced with an increase in the voltage applied to the film.

Based on these experimental results, the two-electrode system ECD (area of 1 cm^2) consisting of the ZnO NWs thin film at the CE and the PB thin film at the WE, was constructed, as depicted in Figure S6. To maintain the electrical neutrality of the PB, 0.5 M KCl aqueous solution as an electrolyte was used. The parameters of the ECD, such as coloration efficiency (η, cm^2/C), transmittance of the coloring state and of the bleaching state (T_c, T_b), switching time, and cycling life, were obtained under the step-wise DC voltage which alternately applies bias at −2.0 and +0.9 V for 10 and 21 s, respectively, as depicted in Figure 3. The η is defined as the change in the optical density (ΔOD) divided by the injected or ejected charge density (Q), represented as follows[36]:

$$\eta = \Delta OD / \Delta Q = \log(T_b/T_c)/\Delta Q$$

The ECD using ZnO NWs thin film shows higher parameter values than all of those from the control ECD with the bare ITO. The results are summarized in Table 1 and depicted in Figure 4. In the case of ECDs with ZnO NWs thin films, η and ΔOD were measured to be 121 cm²/C and 0.4, respectively. Furthermore, the performance of ECDs exhibited slightly degradation within 5% (ΔT) after 1000 switching cycles. ΔT refers to the contrast ratio between T_c and T_b, when the coloration and bleaching states indicated to reach 10% and 90% of its full modulation, respectively. The control ECD with the bare ITO CE had the similar value of η, but the EC phenomenon was not observed after 750 cycles due to the significant deterioration of the electrode materials. The results indicate that the ZnO NWs thin film can play a critical role as an ion storage layer, enabling high EC performance with long life–time of the ECDs.

In summary, we successfully demonstrate that ZnO NW thin film at the CE facilitates enhanced performance of the ECDs. Our study indicates that the concentration of precursors and growth temperature give significant effect on the growth of ZnO NWs structure. The ZnO NWs array was observed to grow vertically when the temperature of the bath was 70°C during electrodeposition under 5 mM ZnCl₂ and 0.1 M KCl. The obtained ZnO NWs by the electrodeposition have a large specific surface area that could play a role of ion storage layer during redox reactions of the PB WE in the ECD. Consequently, the ECD with the ZnO NW thin film exhibited higher coloration efficiency (121 cm²/C) and superior operational stability compared to those from the control ECD. It suggests that ZnO NWs can be a promising candidate of complementary ion storage layer for the development of high-performance ECDs.

Experimental

Reagents and Materials. All the chemical agents used in this study were commercially available and used without further purification. Hydrogen chloride, zinc chloride, potassium chloride, analytical grade $K_3[Fe(CN)_6]$, and $FeCl_3 \cdot 6H_2O$ were purchased from Sigma-Aldrich (Seoul, South Korea).

Electrodeposition of ZnO NWs Thin Films. ZnO NWs thin films on an ITO/glass substrate were prepared in a three-electrode electrochemical cell consisting of a standard calomel electrode (SCE) as the reference electrode, a Pt wire as the CE, and the ITO/glass substrate as the WE. The fabrication of ZnO NWs is followed by two electrodeposition processes. First, ZnO buffer layers were deposited on an ITO/glass substrate by using an electrochemical cell containing an O_2 saturated aqueous solution with 10 mM ZnCl₂ and 0.2 M KCl. The ZnO buffer layers were deposited at −1 V (vs. SCE) room temperature for 1000 s. Second, ZnO NWs were continuously arrayed on the ZnO buffer layers in an electrochemical cell containing an O_2 saturated aqueous solution with 5 mM ZnCl₂ and 0.1 M KCl. The ZnO NWs were deposited at −1 V (vs. SCE) and 70°C for 1000 s (optimal condition). The prepared ZnO

Figure 3. (a) Chronoamperometry curve and the corresponding *in situ* optical transmittance change, and (b) optical transmittance as a function of operation cycles at 700 nm.

Figure 4. (a) Optical transmittance as a function of operation cycles at 700 nm and (b) plot of the transmittance of the ECDs versus number of cycles.

Table 1. EC performances at 700 nm.

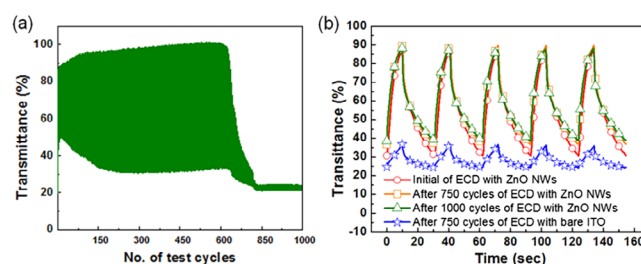|	ΔOD $\log(T_b/T_c)$	η (cm²/C) ($\Delta OD/\Delta Q$)	ΔT (%) (λ: 700 nm)	$\Delta T_{750 \text{ cycles}}$ (%)	$\Delta T_{1000 \text{ cycles}}$ (%)
ECDs with ZnO NWs	0.4	121	48	50	49
Control ECDs with the bare ITO	0.3	120	47	15	-

The configuration of controlled ECDs and ECDs with ZnO NWs is ITO/PB thin film/KCl (0.5 M)/ITO and ITO/PB thin film/KCl (0.5 M)/ZnO NWs/ITO, respectively.

NWs thin films were rinsed using DI water and dried slowly with N_2 to remove water.

Electrodeposition of Prussian Blue Thin Films. PB thin films were deposited on the ITO/glass substrate by chrono-amperometry method in an electrochemical cell, which consists of a three-electrode system (a reference electrode Ag/AgCl, a CE Pt, and a WE ITO/glass substrate) in an aqueous solution containing 0.05 M HCl, 0.05 M $K_3[Fe(CN)_6]$, and 0.05 M $FeCl_3 \cdot 6H_2O$. The PB thin films were subjected to 3 cycles at 0.72–0.77 V at a scan rate of $50\,mVs^{-1}$ for 300 s. The obtained PB thin films were rinsed with DI water and kept away from dust and grease until the experiment was conducted. The average thickness of PB thin films is was 320 nm.

Instruments. Electrochemical experiments were performed using a 650 B electrochemical analyzer (CH Instrument, Austin, TX). The optical properties were measured using UV−vis absorption spectrometry (Bechkman, DU650, Indianapolis, IN). Scanning electron microscopy (SEM, Hitachi S-4300) was used for confirming the thickness of the PB and ZnO NWs thin films. The EC properties including coloration/bleaching, optical density, and coloration efficiency were measured transmittance variation at a wavelength of 700 nm with alternately applied bias at −2.0 and 0.9 V for 10 and 21 s, respectively.

Supporting Information. Additional supporting information may be found online in the Supporting Information section at the end of the article.

References

1. G. Sonmez, C. K. F. Shen, Y. Rubin, F. Wudl, *Angew. Chem. Int. Ed.* **2004**, *43*, 1498.
2. C. M. Amb, A. L. Dyer, J. R. Reynolds, *Chem. Mater.* **2011**, *23*, 397.
3. E. Hwang, S. Seo, S. Bak, H. Lee, M. Lee, H. Lee, *Adv. Mater.* **2014**, *26*, 5129.
4. H. C. Moon, T. P. Lodge, C. D. Frisbie, *Chem. Mater.* **2015**, *27*, 1420.
5. L. M. N. Assis, L. Ponez, A. Januszko, K. Grudzinski, A. Pawlicka, *Electrochim. Acta* **2013**, *111*, 299.
6. R. J. Mortimer, *Annu. Rev. Mater. Res.* **2011**, *41*, 241.
7. D. R. Rosseinsky, R. J. Mortimer, *Adv. Mater.* **2001**, *13*, 783.
8. G. A. Niklasson, C. G. Granqvist, *J. Mater. Chem.* **2007**, *17*, 127.
9. M. Fernandes, V. T. Freitas, S. Pereira, E. Fortunato, R. A. S. Ferreira, L. D. Carlos, R. Rego, V. de Zea Bermudez, *Sol. Energy Mater. Sol. Cells* **2014**, *123*, 203.
10. X. Liu, A. Zhou, Y. Dou, T. Pan, M. Shao, J. Han, M. Wei, *Nanoscale* **2015**, *7*, 17088.
11. Y. −. C. Nah, A. Ghicov, D. Kim, S. Berger, P. Schmuki, *J. Am. Chem. Soc.* **2008**, *130*, 16154.
12. G. −. F. Cai, J. −. P. Tu, J. Zhang, Y. −. J. Mai, Y. Lu, C. −. D. Gu, X. −. L. Wang, *Nanoscale* **2012**, *4*, 5724.
13. K. −. H. Kim, B. −. R. Koo, H. −. J. Ahn, J. Korean, *Mater. Res.* **2018**, *28*, 411.
14. S. Y. Cho, Y. H. Kang, T. −. Y. Jung, S. Y. Nam, J. Lim, S. C. Yoon, D. H. Choi, C. Lee, *Chem. Mater.* **2012**, *24*, 3517.
15. E. L. Runnerstrom, A. Llordés, S. D. Lounis, D. J. Milliron, *Chem. Commun.* **2014**, *50*, 10555.
16. L. Dong, Y. Chu, *Chem. Eur. J.* **2008**, *14*, 5064.
17. M. Regragui, M. Addou, B. El Idrissi, J. C. Bernède, A. Outzourhit, E. Ec–chamikh, *Mater. Chem. Phys.* **2001**, *70*, 84.
18. J. Wang, E. Khoo, P. S. Lee, J. Ma, *J. Phys. Chem. C* **2009**, *113*, 9655.
19. I. Bouessay, A. Rougier, J. Moscovici, A. Michalowicz, J. M. Tarascon, *Electrochim. Acta* **2005**, *50*, 3737.
20. H. Muguerra, G. Berthoux, W. Z. N. Yahya, Y. Kervella, V. Ivanova, J. Bouclé, R. Demadrille, *Phys. Chem. Chem. Phys.* **2014**, *16*, 7472.
21. A. L. Briseno, T. W. Holcombe, A. I. Boukai, E. C. Garnett, S. W. Shelton, J. J. M. Frechet, P. D. Yang, *Nano Lett.* **2010**, *10*, 334.
22. I. Gonzalez-Valls, M. Lira-Cantu, *Energy Environ. Sci.* **2009**, *2*, 19.
23. X. W. Sun, J. X. Wang, *ACS Nano Lett.* **2008**, *8*, 1884.
24. M. Willander, L. L. Yang, A. Wadeasa, S. U. Ali, M. H. Asif, Q. X. Zhao, O. Nur, *J. Mater. Chem.* **2009**, *19*, 1006.
25. J. Wang, L. Zhamg, L. Yu, Z. Jiao, H. Xie, X. W. Lou, X. W. Sun, *Nat. Commun.* **2014**, *5*, 4921.
26. K. −. C. Ho, T. G. Rukavina, C. B. Greenberg, *J. Electrochem. Soc.* **1994**, *141*, 2061.
27. Y. Mastai, D. Gal, G. Hodes, *J. Electrochem. Soc.* **2000**, *147*, 1435.
28. J. Elias, R. Tena–Zaera, C. Lévy–Clément, *Thin Solid Films* **2007**, *515*, 8553.
29. L. Xu, Y. Gou, Q. Liao, J. Zhang, D. Xu, *J. Phys. Chem. B* **2005**, *109*, 13519.
30. S. Yamabi, H. Imai, *J. Mater. Chem.* **2002**, *12*, 3773.
31. M. L. Hitchman, *Measurements of Dissolved Oxygen*, John Wiley & Sons Inc., New York, **1968**.
32. A. Goux, T. Pauporté, J. Chivot, D. Lincot, *Electrhochim. Acta* **2005**, *50*, 2239.
33. R. Tena-Zaera, J. Elias, G. Wang, C. Lévy-Clément, *J. Phys. Chem. C* **2007**, *111*, 16706.
34. J. J. Garcia-Jareno, D. Benito, J. Navarro-Laboulais, F. Vicente, *J. Chem. Ed* **1998**, *75*, 881.
35. A. Dostal, G. Kauschka, S. J. Reddy, F. Scholz, *J. Electroanal. Chem.* **1996**, *406*, 155.
36. J. M. Wang, E. Khoo, P. S. Lee, J. Ma, *J. Phys. Chem. C* **2008**, *112*, 14306.